C-ROADS Technical Reference

Table of Contents

C-ROADS Technical Reference

Last updated June 2025

Lori S. Siegel[1], Chris Campbell[1], Tom Fiddaman[2], Khaled Gaafar[1], Andrew P. Jones[1], Charles Jones[1], John Sterman[3]

[1] Climate Interactive
[2] Ventana Systems
[3] Massachusetts Institute of Technology

The C-ROADS Climate Change Policy Simulator is a climate simulation tool for understanding how we can achieve our climate goals through national and regional commitments. C-ROADS is a globally aggregated model of climate systems linked to regional sectors of emissions and land use. The level of aggregation and several simplifying assumptions allow the model to return results in seconds and be accessible to policy makers and general audiences. C-ROADS is a simple climate model and complements the other, more disaggregated models addressing similar questions, such as integrated assessment models or general circulation climate models. Those larger disaggregated models are used for calibrating results in C-ROADS.

C-ROADS is being developed by Climate Interactive, Ventana Systems, UML Climate Change Initiative, and MIT Sloan.

This *C-ROADS Technical Reference* documents the C-ROADS model structure, equations, assumptions, and data sources. In addition, there is a C-ROADS User Guide more suited to general audiences. For a list of articles about the simulators see our Peer-reviewed Research page. See our training plan for advice on how to use C-ROADS and the World Climate exercise.

Please visit support.climateinteractive.org for additional inquiries and support.

Background

Purpose and Intended Use

C-ROADS stands for Climate-Rapid Overview and Decision Support. It is a rigorous – but rapid and user-friendly – computer simulation of the climate system and its impacts including temperature and sea level rise. C-ROADS is designed to improve understanding of the long-term implications of greenhouse gas emissions and land use decisions.

The climate is a dynamically complex system characterized by feedbacks, time delays, and nonlinear cause-and-effect relationships. Research shows that people misunderstand climate dynamics (Brehmer, 1989; Sterman, 2008); that it is difficult to make decisions in such complex systems (Brehmer, 1989; Kleinmuntz and Thomas,1987; Sterman, 1989); and that computer simulations can help improve decision-making (Morecroft and Sterman, Eds., 1994; Sterman, 2000). Our conversations with stakeholders, such as negotiators tasked with reaching global climate agreements or leaders working to influence those agreements, suggest that even within very high-level policy-making discussions, the ability to understand the aggregate effects of national, regional, or sectoral mitigation commitments on atmospheric CO_2 level and temperature is limited by the scarcity of simple, real-time decision-support tools. The C-ROADS simulator is a tool intended to close this gap.

Thus, the purpose of C-ROADS is to improve public and decision-maker understanding of the long-term implications of international emissions and sequestration futures with a rapid-iteration, interactive tool as a path to effective action that stabilizes the climate. We created C-ROADS to provide a transparent, accessible, real-time decision-support tool that encapsulates the insights of more complex models. The C-ROADS simulator allows for fast-turnaround, hands-on use by decision-makers. It emphasizes:

- Transparency: equations are available, easily auditable, and presented graphically.
- Understanding: model behavior can be traced through the chain of causality to origins; we don't say "because the model says so."
- Flexibility: the model supports a wide variety of user-specified scenarios at varying levels of complexity.
- Consistency: the simulator is consistent with historic data, the structure and insights from larger models, and the Intergovernmental Panel on Climate Change (IPCC) Sixth Assessment Report (AR6).
- Accessibility: the model runs with a user-friendly graphical interface on a laptop computer, in real time.
- Robustness: the model captures uncertainty around the climate outcomes associated with emissions decisions.

C-ROADS is not a substitute for larger integrated assessment models (IAMs) or detailed climate models, such as General Circulation Models (GCMs). Those complex and disaggregated models offer spatial resolution and more details on climate impacts and economic considerations, at a cost of run time, computer power, and opacity. C-ROADS captures some of the key insights from more complex models and makes them available for rapid policy experimentation. Simple models such as C-ROADS complement more disaggregated models, allowing users to gain rapid insights. In turn, larger disaggregated models generate the insights and data used to calibrate and improve the performance of simple models.

C-ROADS is designed to be used interactively with groups as a basis for scientifically rigorous conversations about addressing climate change. It is not intended as a tool for prediction or projections. It is suitable for decision-makers in government, business, and civil society; or for anyone who is curious about the choices of our world.

Overview

The C-ROADS simulator was constructed according to the principles of System Dynamics (SD), which is a methodology for the creation of simulation models that help people improve their understanding of complex situations and how they evolve over time. The method was developed by Jay Forrester at the Massachusetts Institute of Technology in the 1950's and described in his book Industrial Dynamics (Forrester, 1961). SD was the methodology used to create the World3 simulation model that provided the basis for the book The Limits To Growth (Meadows et al., 1972). System dynamics has been described more recently by John Sterman in Business Dynamics (Sterman, 2000).

System dynamics computer simulations, including the C-ROADS simulator, consist of linked sets of differential equations that describe a dynamic system in terms of accumulations (stocks) and changes to those stocks (inflows and outflows). Feedback, delays, and non-linear responses are all included in the simulation. System dynamics simulations help users understand the observed behavior of systems and anticipate future behavior under a variety of scenarios. The C-ROADS simulator is the product of many years of effort, beginning as the graduate research of Tom Fiddaman (Fiddaman, 1997), under the direction of John Sterman, and continued by Tom Fiddaman at Ventana Systems and Lori Siegel, Andrew Jones, and Elizabeth Sawin for Climate Interactive. The simulation model is based on the biogeophysical and integrated assessment literature and includes representations of the carbon cycle, other GHGs, radiative forcing, global mean surface temperature, and sea level change. Consistent with the principles articulated by, e.g., Socolow and Lam, 2007, the simulation is grounded in the established literature yet remains simple enough to run quickly on a laptop computer. Fossil fuel carbon dioxide emissions scenarios for individual nations or groups of nations are aggregated into total fossil fuel CO_2 emissions. These combine with additional uptake and/or release of CO_2 from land use decisions to form the input to the carbon cycle sector of the model. CO_2 concentrations thus determined combine with the influence on net radiative forcing of other well-mixed GHGs (CH_4, N_2O, PFCs, SF_6, and HFCs) via their explicit cycles, to determine the global temperature change, which in turn determines sea level rise.

The model uses country-level historical data through the most recent available data, detailed in Initialization, Calibration, Model Testing.

Baseline CO_2 and other well-mixed gas emissions, population, and GDP default projections are all calibrated to be consistent with the IPCC's SSP2 Baseline scenario in terms of rates yet accounting for divergences in recent years' data from the IPCC projections. Users may change the assumptions driving GDP.

National Aggregation

Scenarios can be created by the user and assessed at three levels of national aggregation.

Table 2.1 Regional Aggregation

Seven Region (7R) Aggregation	Individual Nations
United States (US)	United States (US)
European Union (EU)	Austria, Belgium, Bulgaria, Cyprus, Czech Republic, Denmark, Estonia, Finland, France, Germany, Greece, Hungary, Ireland, Italy, Latvia, Lithuania, Luxemburg, Malta, the Netherlands, Poland, Portugal, Romania, Slovakia, Slovenia, Spain, Sweden
Other Developed Countries 7R	Albania, Andorra, Armenia, Australia, Azerbaijan, Belarus, Bosnia and Herzegovina, Canada, Faeroe Islands, Fiji, Georgia, Gibraltar, Greenland, Holy See, Iceland, Japan, Kazakhstan, Kyrgyzstan, Macedonia, Moldova, Montenegro, New Zealand, Norway, Russian Federation, Serbia, South Korea, Switzerland, Tajikistan, Turkmenistan, Ukraine, United Kingdom, Uzbekistan
China	China
India	India
Other Developing A Countries 7R	Brazil, Indonesia, Hong Kong, Malaysia, Mexico, Myanmar, Pakistan, Philippines, Singapore, South Africa, Taiwan, Thailand
Other Developing B Countries 7R	Afghanistan, Algeria, American Samoa, Angola, Anguilla, Antigua and Barbuda, Argentina, Aruba, Bahamas, Bahrain, Bangladesh, Barbados, Belize, Benin, Bermuda, Bhutan, Bolivia, Botswana, British Virgin Islands, Brunei Darussalam, Burkina Faso, Burundi, Cabo Verde, Cambodia, Cameroon, Central African Republic, Chad, Chile, Colombia, Comoros, Congo, Cook Islands, Costa Rica, Côte d'Ivoire, Croatia, Cuba, Democratic People's Republic of Korea, Democratic Republic of the Congo, Djibouti, Dominica, Dominican Republic, Ecuador, Egypt, El Salvador, Equatorial Guinea, Eritrea, Ethiopia, Falkland Islands (Malvinas), Federated States of Micronesia, French Guiana, French Polynesia, Gabon, Gambia, Germany, Ghana, Grenada, Guatemala, Guinea, Guinea Bissau, Guyana, Haiti, Honduras, Hungary, Iceland, India, Iran, Iraq, Israel, Jamaica, Jordan, Kenya, Kiribati, Kuwait, Lao People's Democratic Republic, Lebanon, Lesotho, Liberia, Libya, Macao, Madagascar, Malawi, Maldives, Mali, Marshall Islands, Mauritania, Mauritius, Mayotte, Mongolia, Montserrat, Morocco, Mozambique, Namibia, Nepal, New Caledonia, Nicaragua, Niger, Nigeria, Niue, Oman, Palau, Panama, Papua New Guinea, Paraguay, Peru, Qatar, Réunion, Rwanda, Saint Helena, Saint Lucia, Samoa, São Tomé and Príncipe, Saudi Arabia, Senegal, Seychelles, Sierra Leone, Slovakia, Slovenia, Solomon Islands, Somalia, Sri Lanka, Sudan, Suriname, Swaziland, Syrian Arab Republic, Timor-Leste, Togo, Tokelau, Tonga, Trinidad and Tobago, Tunisia, Turkey, Turks and Caicos Islands, Tuvalu, Uganda, United Arab Emirates, United Republic of Tanzania, Uruguay, Uzbekistan, Vanuatu, Venezuela, Vietnam, Wallis and Futuna Islands, West Bank and Gaza, Western Sahara, Yemen, Zambia, Zimbabwe

Table 2.2 Six Region Aggregation

Six Region (6R) Aggregation	Individual Nations
United States (US)	US
European Union (EU)	EU
Other Developed Countries 6R	Other Developed Countries 7R
China	China
India	India
Other Developing Countries 6R	Other Developing A Countries 7R, Other Developing B Countries 7R

Table 2.3 Three Region Aggregation

Three Region (3R) Aggregation	Individual Nations
Other Developed Countries 3R	US, EU, Other Developed Countries 7R
Other Developing A Countries 3R	China, India, Other Developing A Countries 7R
Other Developing B Countries 3R	Other Developing B Countries 7R

Notes:

- *Other Developed Countries 7R* includes the Annex I countries within the UNFCCC process; the US and EU are also in the Annex I.
- *Other Developing A Countries 7R* consists of the large developing countries with rising emissions.
- *Other Developing B Countries 7R* consists of smaller developing countries, including the least developed countries and the small island states.

Greenhouse Gas and Climate Structures

The core carbon cycle and climate sector of the model is based on Dr. Tom Fiddaman's MIT dissertation (Fiddaman, 1997).

The model structure draws heavily from Goudriaan and Ketner (1984) and Oeschger and Siegenthaler et al. (1975). The sea level rise sector is based on Rahmstorf, 2007. Temperature feedbacks to the carbon cycle are included, as are the temperature feedbacks to the economy. Model users determine the path of net GHG emissions (CO_2 from FF and land use, CH_4, N_2O, PFCs, SF_6, HFCs, and CO_2 sequestration from afforestation) at the country or regional level, through 2100. The model calculates the path of atmospheric CO_2 and other GHG concentrations, global mean surface temperature, sea level rise, and ocean pH changes resulting from these emissions. The user can choose the level of regional aggregation. Users may choose to provide emissions inputs for one, three, or six different blocs of countries, depending on the purpose of the session. Outputs may be viewed for any of these aggregation levels. Other key variables, such as per capita emissions, and carbon intensity of the economy (e.g., tonnes C per dollar of real GDP), and cumulative emissions, are also displayed. Users can specify the year to stop increasing emissions, the year to start decreasing emissions, and the rate of emissions reductions.

Model Structure

C-ROADS is a system dynamics model. It consists of a set of ordinary differential equations in time. Variables calculated by integration are called “stocks” (also called “levels”); components of the rate of change of a stock are called “flows”; variables used for intermediate steps or calculating other values include auxiliary, constant, data, and initial variables.

Equations represent both physical processes and human decisions. There is no assumption of equilibrium or optimal decision making. The model represents the climate at the global level of aggregation, with emissions and land use for seven regions. The regions are organized into six or three regions, or to the global total, depending on the simulation setting.

C-ROADS is constructed using Vensim modeling software from Ventana Systems, and transformed into an online simulation via the SDEverywhere tools built by Climate Interactive and Todd Fincannon.

C-ROADS is calibrated to an extensive set of historical data, and its endogenous behavior is grounded in and made consistent with other models, in particular the Integrated Assessment Models used by the Intergovernmental Panel on Climate Change (IPCC).

Simulation Method

The differential equations making up C-ROADS are non-linear and have no general closed form solution. Instead they are estimated numerically using the Euler method. At each time step (Δt), auxiliary and flow variables are calculated from previous values of stocks, along with constants and data as needed. Each stock is then computed by adding its previous value to the product of Δt times the sum of all its flows. A sufficiently small time step is required for good approximation - a value of one quarter (0.25) year is appropriate in C-ROADS given the characteristic times and delays in the system as modeled.

C-ROADS starts from initial values in the year 1850 and runs using a combination of data and endogenous behavior through 2100. The model stores and can plot and print the output each year.

Sources of Historical Data

Emissions

- Global Carbon Budget (2023): CO_2 Emissions from fossil fuels
- PRIMAP 2.5.1 (2024): Non-CO_2 GHG Emissions only
- Houghton and Nassikas (2017) (CO_2 Land Use only)

Land Areas

- Land Use Harmonization (LUH2) data (Hurtt et al., 2018)

Population and GDP

- UN World Population Prospects 2024
- World Development Indicators 2024

C-ROADS exogenously uses the historic population, GDP, CO_2 FF emissions, and other GHG emissions. We aggregate these data to import into our data model of 180 countries, which then aggregates those data into the 7 blocs.

Organization

C-ROADS simulator is a synthesis of several sub-models.

- Energy and Industry Emissions;
- Land Use, Land Use Change, and Forestry;
- Terrestrial Biosphere Carbon Cycle;
- Well-Mixed Greenhouse Gas Cycles;
- Climate;
- Sea level rise; and
- Other Impacts.

In the model structure diagrams in the following chapters, there are four types of elements:

1. Variables with a box represent stocks, determined by integration.
2. Variables without a box are auxiliary variables.
3. Simple arrows indicate a causal relationship, one variable is a function of the other.
4. Pipes represent flows - the elements of the rate of change of stocks - shown flowing into, out of, and between stocks.

Energy and Industry Emissions

The Energy and Industry Emissions sector captures the historical and projected CO_2 fossil fuel (FF) emissions for nations or regions and aggregates those emissions into the global CO_2 fossil fuel emissions parameter that serves as input into the carbon cycle sub-model of C-ROADS. The CO_2 Fossil Fuel Emissions variable is the final output of this sector and feeds into the carbon cycle sector. It is determined either by Historical Emissions or Projected CO_2 FF emissions, depending upon the simulated year. The emissions sector has two primary functions within the C-ROADS simulator.

- It aggregates national or regional fossil fuel CO_2 emissions into a single global emissions parameter to feed into the carbon sector sub-model.
- It allows the user to graphically view and compare global CO_2 fossil fuel emissions trajectories and national or regional per capita CO_2 emissions under different scenarios.

Population projections are driven by UN projections; GDP projections are driven by population and GDP per capita; and emissions are driven by GDP and emissions per GDP.Parameters are set so that projections are consistent with the NGFS Current Policies, which are also consistent with the IPCCs AR5 SSP2 RF 6.0.

Reference Scenario Calculation

Population projections also exogenously use those from the UN's medium fertility scenarios for each region.

Projections of GDP are determined by the projected GDP per capita. GDP per capita projections assume growth rates continue from what they are in the period leading up to the last historic year but decrease over time, converging to 1.5% through 2100. GDP is also subject to aggregate economic impact of climate change. Extensive research into the literature shows the vast disparity between estimates of damage at varying temperature changes. We assessed the very low estimates (Nordhaus, 2007, 2013, and 2016; Weitzman, 2012), ranging from 1% at 2 degrees, 2-3 % at 3 degrees, and 4-9% at 4 degrees, and 6-25% at 5 degrees, to be unrealistic. C-ROADS uses the function fitting the Burke et al., (2018) relationship, although the user may turn off the damage effect.

Projections of Baseline emissions, i.e., the Baseline emissions before any actions are implemented, are determined by the projections of emissions per GDP. This structure applies to RS CO_2 FF, CH_4, N_2O, SF_6, PFCs, and HFCs, each with its own starting and convergence rates and times to converge. CO_2 emissions from land use, land use change, and forestry (LULUCF) are detailed in Terrestrial Biosphere Carbon Cycle

Changes to Emissions

Fossil fuel CO_2 emissions grow at the RS rate until a year specified by the user when the growth of emissions stops. Emissions are then held constant until another specified year, when emissions are reduced at an annual rate designated by the user. This allows for the testing of simple scenarios in which the growth, peak, and decline of regional emissions is controlled by the user. The proportional change from the Baseline applies to the Baseline emissions of each GHG.

LULUCF emissions are changed by setting the target action reduce deforestation and degradation. This type of action reduces the land changed or used, which then affects the emissions.

The percent of potential afforestation sets the land converted from other land to forests. Net emissions account for the increase in land removals of CO_2 from the atmosphere.

Land Use, Land Use Change, and Forestry

C-ROADS endogenously calculates the land use, land use change, and forestry (LULUCF) net C emissions by explicitly keeping track of each hectare of different land types; the fluxes of changing land types and the use of each land type due to land and energy demands and policies; and the coflow of carbon on the land. The land area is disaggregated by land type, denoted with a "u" suffix, and by region, denoted by an "r" suffix. Variables reflecting a change from one type of land to another type for a given region has the suffix "uur".

The terrestrial biosphere carbon (TBC) cycle accounts for these anthropogenic carbon emissions as well as natural emissions from biomass and soil respiration and releases as CH_4, accounted in the CH_4 cycle, and primary productivity of each land type.

The TBC cycle reflects that cutting down trees releases carbon, and stops the them from absorbing CO_2 from the atmosphere. While harvesting crops also releases carbon, the approximately annual or faster regrowth time allows the related carbon release to be considered net zero.

C-ROADS models different kinds of land that can be converted into the others, and the biomass and soil carbon on the land that can build up or be released. We have four different land uses: Forest, Agriculture, Other, Tundra; with Forest further divided into three cohorts (Young, 0-50 years; Medium, 50-100 year; and Mature, 100+ years) and whether or not it resulted from afforestation (9 total land uses).

Each type of land has carbon flows:

- From the atmosphere to biomass (primary production through photosynthesis)
- From biomass to soil (decomposition et cetera)
- From soil and biomass to the atmosphere (respiration, decay, burning)
- When land use changes, some of the carbon stays on the land and some is released to the atmosphere

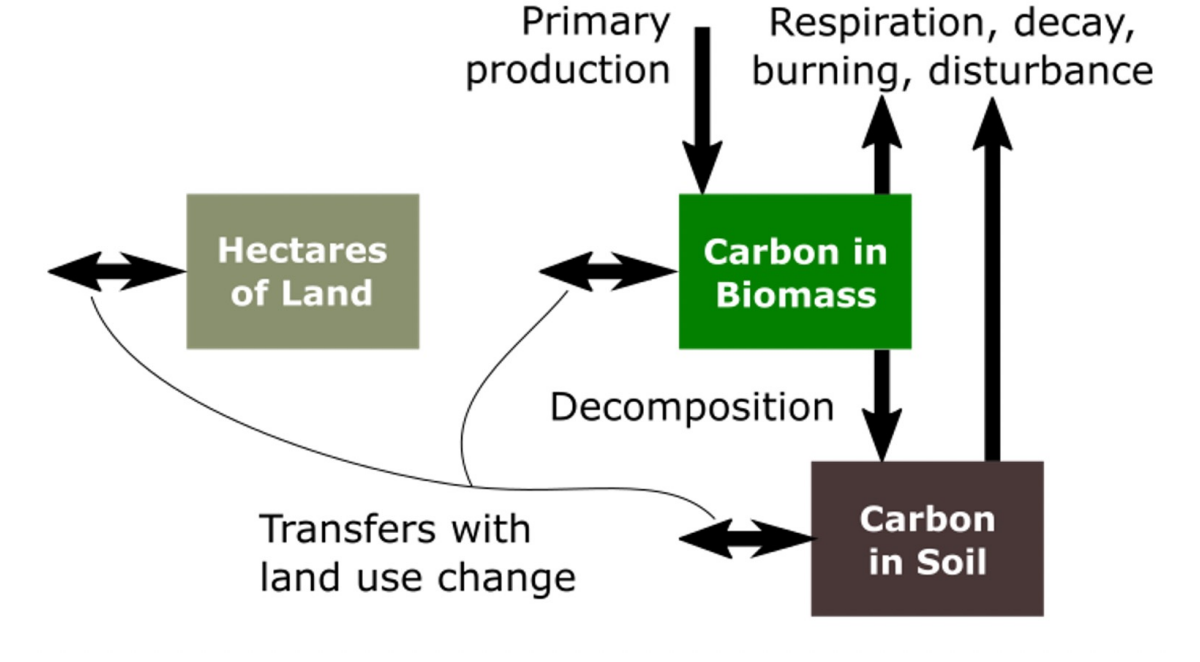

Figure 5.1 Land and Carbon Stock and Flow

We cut trees or remove biomass for two reasons: we want the material or we want the land (or both). The material is involved in concepts like bioenergy, wood products, and forest degradation. Needing the land means concepts like deforestation, afforestation, land use change, and agriculture. Those are the policies and scenarios where you can intervene in En-ROADS with each area described below.

Drivers of Deforestation and Degradation

Land that is converted from forest becomes either Farmland (driven by needs of the food system and bioenergy) or Other Land (non-farm deforestation). With six subcategories of forest (NonAF/AF, Young/Medium/Mature), the model assumes that the fraction of deforestation to farmland and to other is proportional to the land area of each to the total forest land.

The primary driver of deforestation has historically been to expand farmland to meet food demands and by the fraction of farmland expansion that comes from forest. Farmland needs that cannot come from forest comes from Other Land. Farm conversion from other land (mostly grasslands and scrub, but also deserts, barren, urban, etc) has less effect on the carbon cycle than does deforestation. The fraction of farmland expansion that comes from forest is fixed (at 0.6) in the base case based on historical land use changes.

Deforestation to other land reflects forest clearing for development and mining.

A data model uses the LUH land area data and projections from SSP2, aggregated to 20 regions, to determines the land areas changes per year. These land area changes are aggregated to the 7 regions used in C-ROADS. The resulting fluxes are set as default land changes in the model.

Forests are also harvested for bioenergy and for non-fuel wood (lumber, paper, et cetera), and allowed to regrow. Both fuel and non-fuel wood demand for each region are based on history and projections are based on continuing the per capita demand times the population. The regrowing process can remove carbon from the atmosphere and is therefore often considered carbon-neutral. However, it can take decades to repay the carbon debt incurred with forest harvesting. All forests can be harvested for bioenergy or for wood products. The proportion of total harvest from each forest category is a function of available carbon on each category relative to the total carbon on all forests.

The policy to prevent deforestation reduces both deforestation and degradation from the mature forest cohort.

Other Land Decreases and Increases

Afforestation policy, i.e. the action depending on the Afforestation slider of En-ROADS, is implemented as the conversion of other land to forest land, since the land identified to be available for afforestation , excludes existing forests and agricultural land and falls into the other land category. Afforestation, as a policy implementation, is formulated based on a user-defined fraction of the full potential of afforestable land, and its delayed conversion to afforested land, which results in the land flux of Land afforestation rate. This flux is then incorporated into the land use change module as a chain of conversions from the other land to young forests and then aging to medium and mature forests. Deforestation from afforested land to farmland and other land affects the efficacy of this policy. The model captures historic regrowth of other land to nonAF young forest. Other land also decreases with farmland expansion, as only a fraction of the expansion comes from forests.

Model Structure

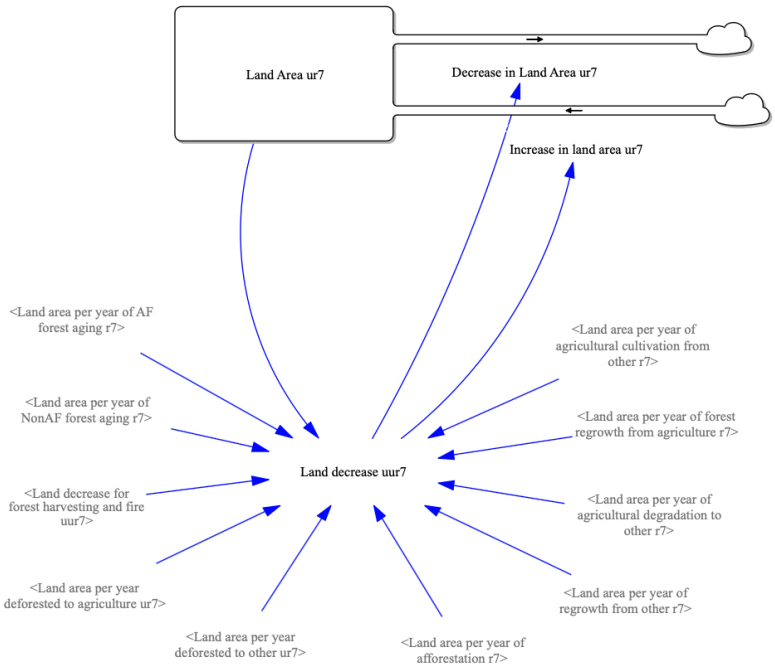

Figure 5.2 Land Use Change Structure

Terrestrial Biosphere Carbon Cycle

The terrestrial biosphere carbon (TBC) cycle reflects the primary productivity of biomass, removing carbon from the atmosphere as it grows, the natural and anthropogenic carbon fluxes from biomass and soil stocks, the flux from biomass carbon to soil carbon, and the fluxes of biomass and soil carbon as methane to the methane cycle. These fluxes by land type are summed together to feed into the carbon cycle.

The Goudriaan and Ketner and IMAGE models (Goudriaan and Ketner, 1984; Rotmans, 1990) have detailed biospheres, partitioned into leaves, branches, stems, roots, litter, soil, and charcoal. To simplify the model, these categories are aggregated into stocks of biomass (leaves, branches, stems, roots) and soil (litter, soil). First-order time constants were calculated in C-ROADS assuming equilibrium in 1850 for each category land type and C-ROADS region and aggregated across regions for use in En-ROADS. Charcoal is neglected due to its long lifetime. The results are reasonably consistent with other partitionings of the biosphere and with the one-box biosphere of the Oeschger model (Oeschger, Siegenthaler et al., 1975; Bolin, 1986).

Net Primary Productivity (NPP)

The natural ability of biomass to sequester carbon from the atmosphere provides a key sink in the carbon cycle. NPP is the gross primary productivity minus the autotrophic respiration. Forest, agricultural land, other land, and tundra all have primary production and respiration. Furthermore, all primary production is affected by the level of CO_2 in the atmosphere (the fertilization effect). Carbon stored in biomass and soil is also released through heterotrophic aerobic and anaerobic respiration, which increases with higher temperature (increased fire, pests, decay). With the major exception of forests, all land reaches equilibrium quickly. Accordingly, the initial unit NPP of each nonforest land type is set assuming equilibrium in 1850. The flux into the biomass is equal to the flux out from aerobic and anaerobic respiration and transfer to soil is divided by the land area.

Unlike the other land types, forests have the most complex growth and the most biomass, so are treated in the most detail. Trees take up carbon through photosynthesis / primary production, and lose it through respiration, fire, being eaten by animals, decay, et cetera. Some of the carbon lost from biomass ends up in the soil through decomposition. The net of these carbon flows is that forests grow in an S-shaped pattern, slowly at first, at a high rate in middle age, and then reach an equilibrium where very high primary production is balanced by very high respiration. The growth curves, primary production, respiration and soil transfer rates are initialized and calibrated with land use harmonization (LUH), and OSCAR modeling output and compared against Houghton and Nassikas (2017) and SSP IAMs.

- Initialize carbon in stocks of forest, farmland, tundra, and other biomass and soil from OSCAR 1850 output by 10 regions, disaggregated and re-aggregated to fit our 7 regions.
- Initialize fractional rate of biomass and soil C respiration and transfer biomass to soil from OSCAR 1850 output.
- Determine forest unit NPP Richard's growth curve parameters for each of 7 regions.
    - Set Test Pulse scenario in which all LULUCF is set to 0 EXCEPT for a pulse of 95 of mature forest in 1900; when Test Pulse = 1, all fertilization and temperature feedbacks are turned off.
    - Set unit NPP inputs within ranges determined from forest analyses and assure unit NPP curves are reasonable given the types of forests in each region, e.g., more tropical in India and Other Developing A and B and more temperate in Developed.

- Iteratively adjust parameters to achieve near equilibrium prior to pulse and assure regrowth is reasonable given the types of forests in each region.

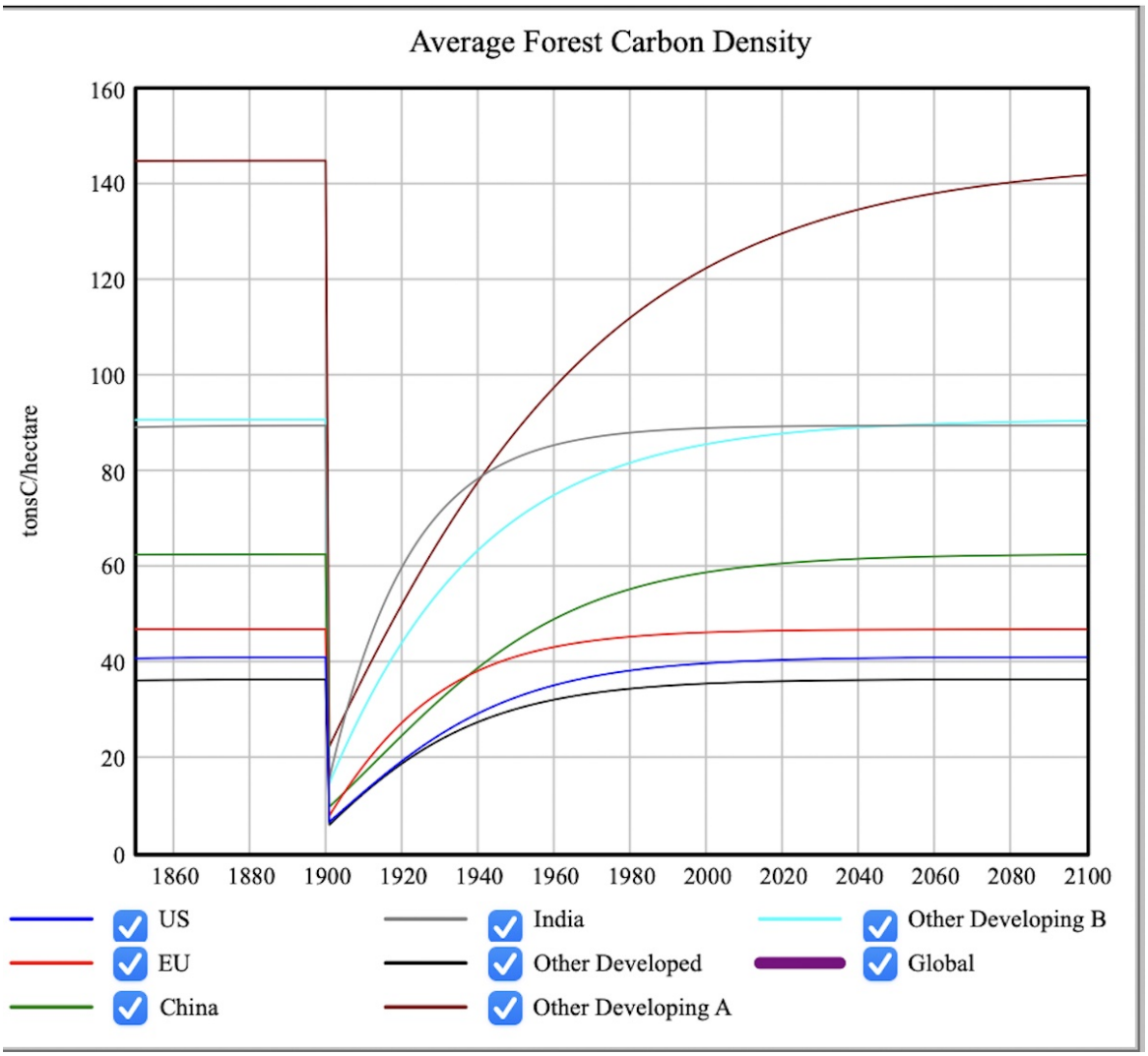

Figure 6.1 Regrowth After Instant Deforestation

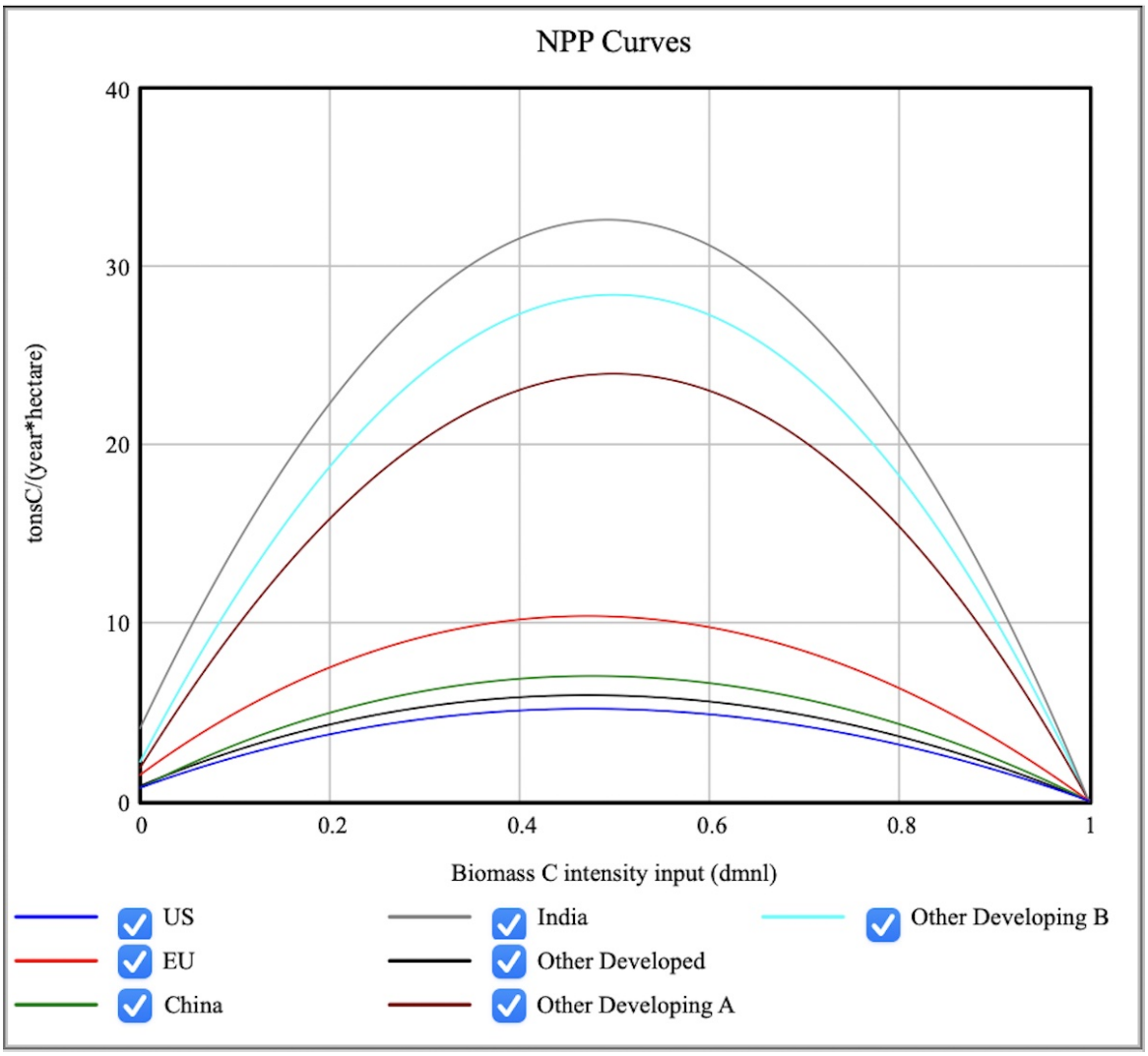

Figure 6.2 Net Primary Productivity versus Biomass Density

The logarithmic relationship of the uptake of C by the biosphere reflects the fact that the uptake is less than proportional to the increase in atmospheric C concentration (Wullschleger, Post et al., 1995). This formulation, though commonly used, is not robust to large deviations in the atmospheric concentration of C. As the atmospheric concentration of C approaches zero, net primary production approaches minus infinity, which is not possible given the finite positive stock of biomass. As the concentration of C becomes very high, net primary production can grow arbitrarily large, which is also not possible in reality. Accordingly, we instead use a CES production function, which exhibits the following: 1) the slope around the preindustrial operating point is controlled by the biostimulation coefficient, which can be loosely interpreted as CO_2's share of plant growth (at the margin), with the balance due to other factors like water and nutrients; 2) there is a finite slope at zero CO_2, such that there are no singularities; and 3) it controls saturation at high CO_2.

$$NPP = NPP_0 \left(1 - \beta_b + \beta_b \frac{C_a}{C_{\mathrm{a},0}}^{CO_2 \cdot sat}\right)^{\frac{1}{CO_2 \cdot sat}}$$

NPP = net primary production
NPP_0 = reference net primary production
β_b = biostimulation coefficient
C_a = C in atmosphere
$C_{a,0}$ = reference C in atmosphere
$CO_2 \cdot sat$ = coefficient that determines the rate of CO_2 saturation

Natural Losses

Carbon stored in biomass and soil is lost due to fire and microbial/fungal respiration. Rates of the release from each carbon stock is increased with increasing temperature change.

Carbon in both biomass and soil is also released as natural methane, entering into the methane cycle as such. The fractional rates of these releases also increase with temperature change. We assume a linear relationship, likely a good approximation over the typical range for warming by 2100. The sensitivity parameter, set by the user, governs the strength of the effect. The default sensitivity of 1 yields the average value found in Friedlingstein et al., 2006. Additionally, the rate of methane from tundra increases as temperature exceeds a threshold, representing a tipping point in the model.

Anthropogenic Carbon Fluxes

Land Use, Land Use Change, and Forestry explains the land use changes and uses. Carbon emitted from LUC is a coflow of each land change, driven by the Fraction biomass C emitted and Fraction soil C emitted. The remaining carbon, i.e., 1 minus that fraction, drives the carbon transferred to the new land type.

Net removals from regrowth after harvesting and from afforestation account for the net primary productivity (NPP) and also for the carbon lost back to the atmosphere from aerobic and anaerobic respiration and to the carbon and methane cycles, respectively. In order to isolate the removals due to land changes, the model simultaneously calculates the removals for the counterfactual scenario of no land changes. Corresponding coflows, aerobic and anaerobic respiration, and transfers from biomass to soil drive the TBC cycle without harvesting and regrowth. Accordingly, the net removals due to land changes are taken as difference in net removals with and without the land changes.

The net carbon emissions from LULUCF are the gross emissions, i.e., the LULUCF released to the atmosphere from biomass and soil, minus the net removals due to the land changes.

A reduction in converting forests and in harvesting mature trees leads to a reduction in net emissions from LULUCF, eventually meaning negative emissions. Part of this is because bioenergy from wood falls - the young and medium forests cannot make up for the reduced availability of biomass from mature forests, which makes wood more expensive. Increases from the other sources of biomass (crops and waste) only partially cover the reduction from wood.

Bioenergy

The amount of bioenergy used is based on the wood used for bioenergy in En-ROADS. In turn, harvesting for bioenergy removes the indicated carbon, converting any age of forest into new forest with low carbon content, or increasing the desired farmland.

LULUCF net emissions are reported in two ways, including those resulting from bioenergy and also excluding those when reporting bioenergy emissions are reported separately. Regardless of reporting, bioenergy emissions and resulting net removals are appropriately included in the TBC cycle and included as such in the main carbon cycle. Although reported as part of the energy emissions, bioenergy net emissions are not included with the Global C energy and industry emission flux of carbon into the atmosphere.

All forests supply bioenergy and wood for non-fuel products according to their carbon content. To isolate the removals due to harvesting for bioenergy, the model also calculates the counterfactual land areas and terrestrial biosphere carbon resulting from all fluxes excluding harvest and regrowth for bioenergy.

Forest Fires

Forest fires are emphasized due to the role of forests as carbon sinks and their slow regeneration post-burning. Shrub and grassland fires are considered carbon-neutral due to their rapid vegetation recovery.

Historical data from the Global Wildfire Information System (GWIS) database shows a steady decline in total annual wildfire burned area between 2002-2023 with forest fire burned area declining at a much slower rate compared to other vegetation types. Historical data from Global Forest Watch (GFW) shows a steady rise in severe ‘stand-replacing’ forest fires between 2001-2023 posing a threat to forest recovery. Furthermore, analysis by Jones et al. (2024) concludes that severe forest fires have been annually increasing, both in area and in intensity, over the past 2 decades particularly in areas where forest fires are linked to climate change.

Forest fires induced by climate change are explicitly modeled, estimated as a percentage of projected total forest area. Forest fires not induced by climate change are accounted for in the calculations of natural losses. Similar to natural losses, the rate of release from biomass and soil carbon stocks due to forest fires is increased with increasing temperature change.

Forest fires release CO_2 and methane into the atmosphere, contributing to temperature change, which feeds back to increase annual burned area. Mature and medium-aged forests experiencing fires degrade into young forests, and a portion of forest burned area is severely damaged to the extent that it cannot regrow. This deforestation effect is considered to be a subcategory of stand-replacing forest fires.

There is uncertainty on the impact of temperature change on wildfires in general, and on forest fires specifically. Literature such as Lange et al. (2020), and analysis of results from Knorr et al. (2016), suggests a strong linear effect of increasing temperature on annual wildfire burned area. This effect is estimated combining results from the literature with data from the GWIS database of historical wildfire area. Furthermore, there is uncertainty on the proportion of 'stand-replacing' burned area that is deforested. Data from GWIS and GFW were used to estimate the relationship between temperature and the proportion of forest fires that cause tree cover loss. Literature and expert judgement were leveraged to estimate the fraction of stand-replacing fires that cause permanent tree cover loss.

Well-Mixed Greenhouse Gas Cycles

Carbon Cycle

Introduction

The carbon cycle sub-model is adapted from the FREE model (Fiddaman, 1997). While the original FREE structure is based on primary sources that are now somewhat dated, we find that they hold up well against recent data. Calibration experiments against recent data and other models do not provide compelling reasons to adjust the model structure or parameters, though in the future we will likely do so.

Other models in current use include simple carbon cycle representations. Nordhaus' DICE models, for example, use simple first- and third-order linear models (Nordhaus, 1994, 2000). The first-order model is usefully simple, but does not capture nonlinearities (e.g., sink saturation) or explicitly conserve carbon. The third-order model conserves carbon but is still linear and thus not robust to high emissions scenarios. More importantly for education and decision support, neither model provides a recognizable carbon flow structure, particularly for biomass.

Socolow and Lam (2007) explore a set of simple linear carbon cycle models to characterize possible emissions trajectories, including the effect of procrastination. The spirit of their analysis is similar to ours, except that the models are linear (sensibly, for tractability) and the calibration approach differs. Socolow and Lam calibrate to Green's function (convolution integral) approximations of the 2x CO_2 response of larger models; this yields a calibration for lower-order variants that emphasizes long-term dynamics. Our calibration is weighted towards recent data, which is truncated, and thus likely emphasizes faster dynamics. Nonlinearities in the C-ROADS carbon uptake mechanisms mean that the 4x CO_2 response will not be strictly double the 2xCO_2 response.

Structure

The adapted FREE carbon cycle is an eddy diffusion model with stocks of carbon in the atmosphere, biosphere, mixed ocean layer, and three deep ocean layers. The model couples the atmosphere-mixed ocean layer interactions and net primary production of the Goudriaan and Kettner and IMAGE 1.0 models (Goudriaan and Ketner 1984; Rotmans 1990) with a 5-layer eddy diffusion ocean based on (Oeschger, Siegenthaler et al., 1975) and a 2-box biosphere based on (Goudriaan and Ketner 1984).

The global terrestrial biosphere carbon cycle fluxes and initial biomass and soil stocks are the sum of those by land type as defined in Terrestrial Biosphere Carbon Cycle.

The interaction between the atmosphere and mixed ocean layer involves a shift in chemical equilibria (Goudriaan and Ketner, 1984). CO_2 in the ocean reacts to produce HCO_3^- and $CO_3^=$. In equilibrium,

$$C_m = C_{\mathrm{m},0}\left(\frac{C_a}{C_{\mathrm{a},0}}\right)^{\frac{1}{\zeta}}$$

C_m = C in mixed ocean layer
$C_{m,0}$ = reference C in mixed ocean layer
C_a = C in atmosphere
$C_{a,0}$ = reference C in atmosphere
ζ = buffer factor

The atmosphere and mixed ocean adjust to this equilibrium with a time constant of 1 year. The buffer or Revelle factor, ζ, is typically about 10. As a result, the partial pressure of CO_2 in the ocean rises about 10 times faster than the total concentration of carbon (Fung, 1991). This means that the ocean, while it initially contains about 60 times as much carbon as the preindustrial atmosphere, behaves as if it were only 6 times as large.

The buffer factor itself rises with the atmospheric concentration of CO_2 (Goudriaan and Ketner, 1984; Rotmans, 1990) and temperature (Fung, 1991). This means that the ocean's capacity to absorb CO_2 diminishes as the atmospheric concentration rises. This temperature effect is another of several possible feedback mechanisms between the climate and carbon cycle. The fractional reduction in the solubility of CO_2 in ocean falls with rising temperatures. Likewise for the temperature feedback on C flux to biomass, we assume a linear relationship, likely a good approximation over the typical range for warming by 2100. The sensitivity parameter that governs the strength of the effect on the flux to the biomass also governs the strength of the effect on the flux to the ocean. For both effects, the default sensitivity of 1 yields the average values found in Friedlingstein et al., 2006.

$$\zeta = \zeta_0 + \delta_b \ln\left(\frac{C_a}{C_{\mathrm{a},0}}\right)$$

ζ = buffer factor
ζ_0 = reference buffer factor
δ_b = buffer CO_2 coefficient
C_a = C in atmosphere
$C_{a,0}$ = reference C in atmosphere

The deep ocean is represented by a simple eddy-diffusion structure similar to that in the Oeschger model, but with fewer layers (Oeschger, Siegenthaler et al., 1975). Effects of ocean circulation and carbon precipitation, present in more complex models (Goudriaan and Ketner, 1984; Björkstrom, 1986; Rotmans, 1990; Keller and Goldstein, 1995), are neglected. Within the ocean, transport of carbon among ocean layers operates linearly. The flux of carbon between two layers of identical thickness is expressed by:

$$F_{\mathrm{m,n}} = \frac{(C_m - C_n)^e}{d^2}$$

$F_{m,n}$ = carbon flux from layer *m* to layer *n*
C_k = carbon in layer *k*
e = eddy diffusion coefficient
d = depth of layers

The effective time constant for this interaction varies with d, the thickness of the ocean layers. To account for layer thicknesses that are not identical, the time constant uses the mean thickness of two adjacent layers. The following table summarizes time constants for the interaction between the layers used in C-ROADS, which employs a 100 meter mixed layer, and four deep ocean layers that are 300, 300, 1300, and 1800 meters, sequentially deeper. Simulation experiments show there is no material difference in the atmosphere-ocean flux between the five-layer ocean and more disaggregate structures, including an 11-layer ocean, at least through the model time horizon of 2100.

Table 7.1 Effective Time Constants for Ocean Carbon Transport

Layer Thickness	Time Constant
100 meters	1 year
300 meters	14 years
300 meters	20 years
1300 meters	236 years
1800 meters	634 years

The carbon cycle also includes removals from carbon dioxide removal (CDR) technologies and any leak or loss rates from storage.

Other greenhouse gases

Other GHGs included in CO_2equivalent emissions

C-ROADS explicitly models other well–mixed greenhouses gases, including methane (CH_4), nitrous oxide (N_2O), and the fluorinated gases (PFCs, SF_6, and HFCs). PFCs are represented as CF_4-equivalents due to the comparably long lifetimes of the various PFC types. HFCs, on the other hand, are represented as an array of the nine primary HFC types, each with its own parameters. The structure of each GHG's cycle reflects first order dynamics, such that the gas is emitted at a given rate and is taken up from the atmosphere according to its concentration and its time constant. Initialization is based on data from GISS for CH_4, N_2O, and PFCs, and assumed zero for SF_6 and HFCs. The remaining mass in the atmosphere is converted, according to its molecular weight, to the concentration of that gas. The multiplication of each gas concentration by the radiative coefficient of the gas yields its instantaneous radiative forcing (RF). This RF is included in the sum of all RFs to determine the total RF on the system.

For those explicitly modeled GHGs, the CO_2 equivalent emissions of each gas are calculated by multiplying its emissions by its 100-year Global Warming Potential. Time constants, radiative forcing coefficients, and the GWP are taken from the IPCCs Fifth Assessment Report (AR5) Working Group 1 Chapter 8. (Table 8.A.1. Lifetimes, Radiative Efficiencies and Metric Values GWPs relative to CO_2).

For those explicitly modeled GHGs, the CO_2 equivalent emissions of each gas are calculated by multiplying its emissions by its 100-year Global Warming Potential. Time constants, radiative forcing coefficients, and the GWP are taken from the IPCCs Fifth Assessment Report (AR5) Working Group 1 Chapter 8. (Table 8.A.1. Lifetimes, Radiative Efficiencies and Metric Values GWPs relative to CO_2).

In addition to the anthropogenic emissions considered as part of the CO_2 equivalent emissions, CH_4, N_2O, and PFCs also have a natural component. The global natural CH_4 emissions are from the anaerobic respiration of biomass, soil, and oceans. The global natural N_2O emissions are based on MAGICC output, using the remaining emissions in their "zero emissions" scenario. The global natural PFC emissions are calculated by dividing Preindustrial mass of CF_4 equivalents by the time constant for CF_4. Figure 7.2 illustrates the general GHG cycle. The units of each gas are: MtonsCH_4, MtonsN_2O-N, tonsCF_4, tonsSF_6, and tonsHFC for each of the primary HFC types. To calculate the CO_2 equivalent emissions of N_2O, the model first converts the emissions from MtonsN_2O-N/year to Mtons N_2O/year.

CH_4 is unique in that there are additional natural emissions from permafrost and clathrate. The sensitivity of this release defaults to 0.1% per degree Celsius over a threshold, defaulted to 2 Degrees Celsius; the user may change these assumptions.

Montréal Protocol Gases

Rather than explicitly modeling the cycles of the Montreal Protocol (MP) gases, whose emissions are dictated by the MP, En-ROADS uses the calculated RF for historical and projected concentrations, inputted as a data variable.

Cumulative Emissions

C-ROADS calculates the cumulative CO_2 with the initial value taken as the 1990 C-ROADS value starting in 1870. Cumulative emissions are determined through the simulation. The trillionth ton is a marker of cumulative emissions above which a two degree future is far less likely. Budgets are also presented from 2011 and from 2018, based on IPCC thresholds.

Model Structure

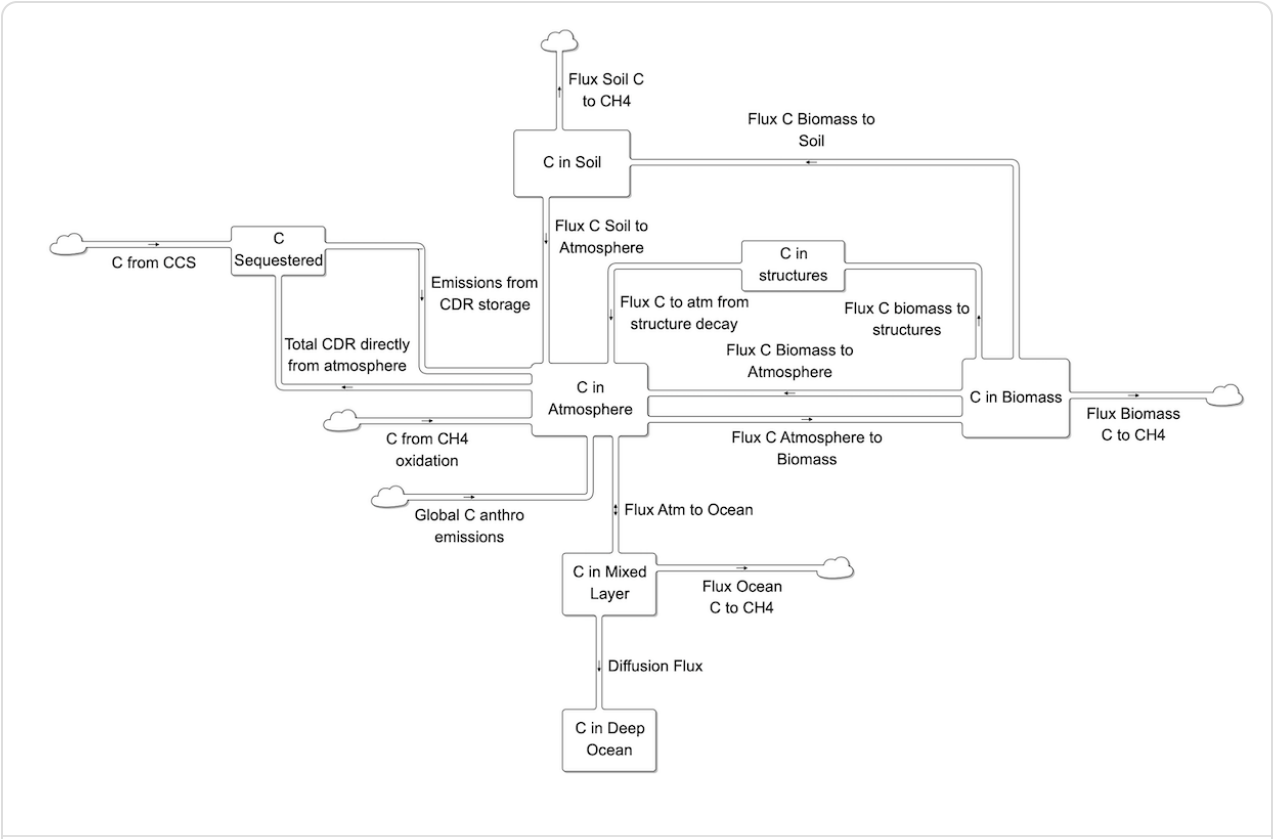

Figure 7.1 C-ROADS Carbon Cycle Structure

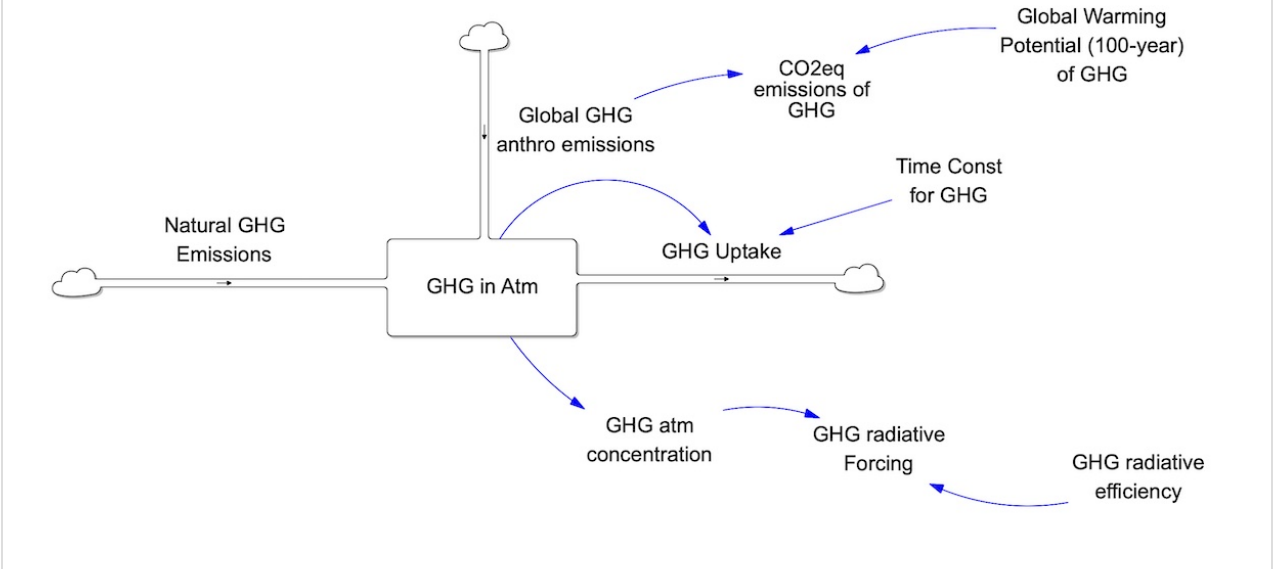

Figure 7.2 C-ROADS Other GHGs Cycle Structure

Climate

Introduction

Like the carbon cycle, the climate sector is adapted from the FREE model, which used the DICE climate sector without modification (Nordhaus 1994). The DICE structure in turn followed Schneider and Thompson (1981).

The model has been recast in terms of stocks and flows of heat, rather than temperature, to make the physical process of accumulation clearer to users. However, the current model is analytically equivalent to the FREE and DICE versions. While FREE and DICE used exogenous trajectories for all non-CO_2 radiative forcings, this version adds endogenous forcings from all well-mixed GHGs, i.e., CO_2, CH_4, N_2O, PFCs, SF_6, and each HFC type.

Structure

The model climate is a fifth-order, linear system, with three negative feedback loops. Two loops govern the transport of heat from the atmosphere and surface ocean, while the third represents warming of the deep ocean. Deep ocean warming is a slow process, because the ocean has such a large heat capacity. If the deep ocean temperature is held constant, the response of the atmosphere and surface ocean to warming is first-order. Temperature change is a function of radiative forcing (RF) from greenhouse gases and other factors, feedback cooling from outbound longwave radiation, and heat transfer from the atmosphere and surface ocean to the deep ocean layer.

$$
\begin{aligned}
T_{\text{surf}} &= \frac{Q_{\text{surf}}}{R_{\text{surf}}} \\
T_{\text{deep}} &= \frac{Q_{\text{deep}}}{R_{\text{deep}}} \\
Q_{\text{surf}} &= \int \left(RF(t) - F_{\text{out}}(t) - F_{\text{deep}}(t)\right) dt + Q_{\text{surf}}(0) \\
Q_{\text{deep}} &= \int F_{\text{deep}}(t)\, dt + Q_{\text{deep}}(0)
\end{aligned}
$$

T = temperature of surface and deep ocean boxes
Q = heat content of respective boxes
R = heat capacity of respective boxes
RF = radiative forcing
F_{out} = outgoing radiative flux
F_{deep} = heat flux to deep ocean

$$F_{\text{out}}(t) = \lambda T_{\text{surf}}$$

$$F_{\text{deep}}(t) = R_{\text{deep}} \cdot \frac{T_{\text{surf}} - T_{\text{deep}}}{\tau}$$

λ = climate feedback parameter
τ = heat transfer time constant

Radiative forcing from CO_2 is logarithmic of the atmospheric CO_2 concentration (IPCC AR6, 2023; NOAA, 2024). Forcing from CH_4 and N_2O is less than the sum of RF from each individually to account for interactions between both gases. Forcing from each F-gas is the product of its concentration and its radiative forcing coefficient; the total forcings of F-gases is the sum of these products, as are the forcings from MP gases derived. The sum of other forcings, which include those from aerosols (black carbon, organic carbon, sulfates), tropospheric ozone, defaults to an exogenous time-varying parameter. The values use a composite of AR6 history 1750-2019 and their projections for SSP4 6.0 through 2100. The equilibrium temperature response to a change in radiative forcing is determined by the radiative forcing coefficient, κ, and the climate feedback parameter, λ. Equilibrium sensitivity to 2xCO_2eq forcing is 3°C in the base case.

$$T_{\text{equil}} = \frac{\kappa \cdot ln\left(\frac{C_a}{C_{a,0}}\right)}{\lambda \cdot ln(2)}$$

T_{equil} = equilibrium temperature
C_a = atmospheric CO_2 concentration
$C_{a,0}$ = preindustrial atmospheric CO_2 concentration
κ = radiative forcing coefficient
λ = climate feedback parameter

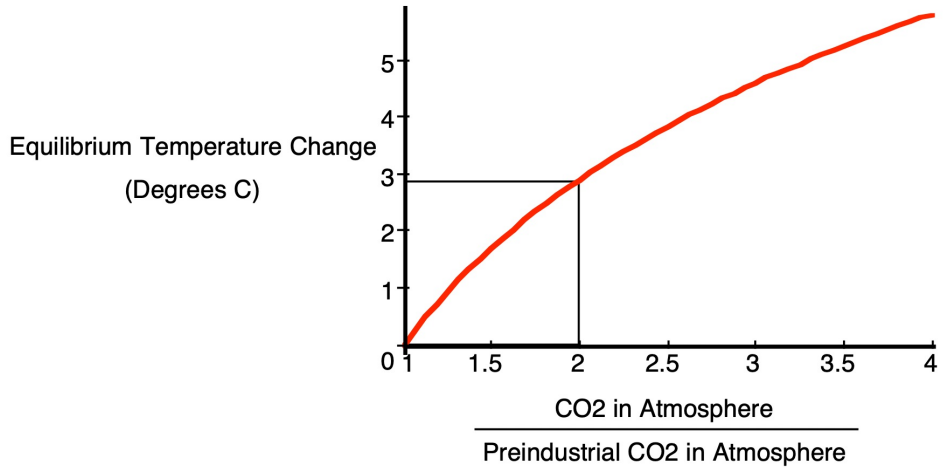

Figure 8.1 Equilibrium Temperature Change versus CO_2 Concentration

Model Structure

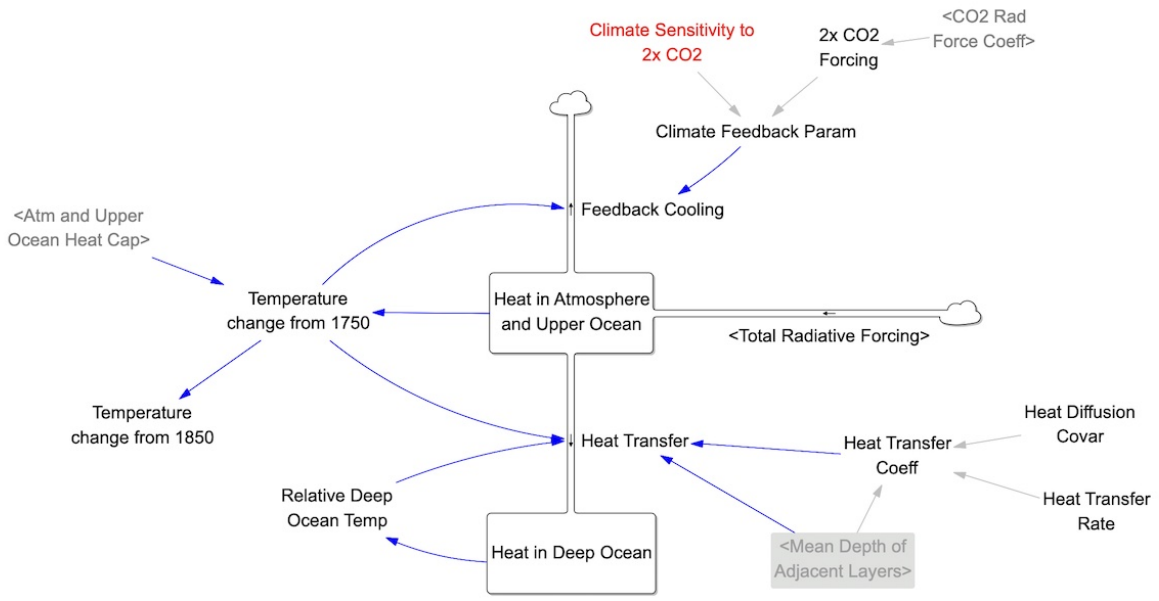

Figure 8.2 Heat Transfer Model Structure

Sea Level Rise

SLR is modeled by extending the semi-empirical approach proposed by Vermeer and Rahmstorf (2009) in a way to accommodate the water impoundment by artificial reservoirs and to experiment with higher levels of contribution to SLR from ice sheet melting in Antarctica and Greenland than already assumed. The model is estimated from historical data 1900-2021, a period with low levels of warming that therefore may underestimate future sea level rise from the faster-than-historical rates of melt of the Greenland and Antarctic ice sheets. “Contribution to SLR from Ice Melt in Antarctica by 2100” and “Contribution to SLR from Ice Melt in Greenland by 2100” sliders allow users to capture these effects. Sliders are initialized with the mid-range estimates for the contribution of ice sheet melting in Antarctica/Greenland in the IPCC AR6 report.

Model Structure

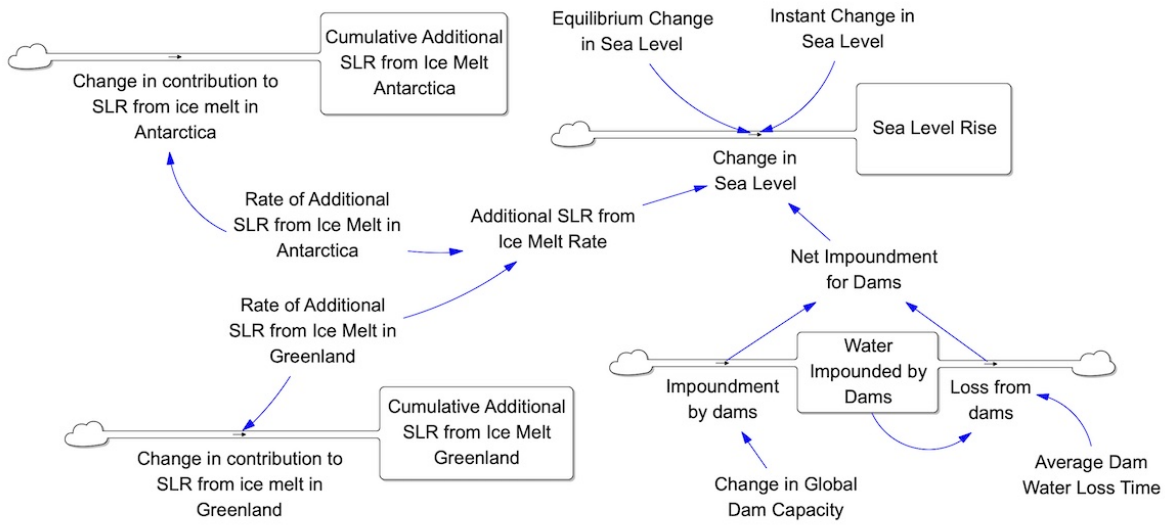

Figure 9.1 En-ROADS Sea Level Rise Model Structure

Other Impacts

pH

The pH sector of En-ROADS reflects the empirical function presented by Bernie et al. (2010). As the atmospheric concentration in the atmosphere increases, the pH of the ocean decreases by a third order response.

Other Impacts from Temperature Change

The continuous increase in the global temperature is expected to cause a variety of impacts on ecology and human activities – in addition to sea level rise, increased ocean acidity and the loss in global GDP discussed in previous sections. More frequent and intense extreme weather events, major reduction in global crop yield and biodiversity loss are some examples of the other anticipated impacts of climate change. En-ROADS simulates five categories of such climate impact metrics (some categories containing more than one metric):

- Population Exposed to Sea Level Rise
- Probability of Ice-free Arctic Summer
- Decrease in Crop Yield from Temperature
- Species Losing More than 50% of Climatic Range
- Additional Deaths from Extreme Heat

Building on the findings of five peer-reviewed climate studies, we formulated the relationship between global mean temperature (as well as sea level rise) and these metrics, primarily through interpolation and extrapolation.

Initialization, Calibration, Model Testing

C-ROADS initializes and calibrates to available historical data, primarily provided by the following sources:
Greenhouse Gas Emissions

- Global Carbon Budget (2023) (CO_2 Energy Emissions and Land Use Change Emissions)
- PRIMAP 2.5.1 (2024) (Non-CO_2 GHG Emissions only)
- Houghton and Nassikas (2017) (CO_2 Land Use only)

Land Areas

- Land Use Harmonization (LUH2) data (Hurtt et al., 2018)

GHG Concentrations, Temperature Change, Sea Level Rise

- National Oceanic and Atmospheric Administration (NOAA) concentrations (2025) and radiative forcings (2023)
- GISS Global Mean Estimates based on Land and Ocean Data 1880-2023 (2024)
- HadCRUT5 1850-2023 (2024)
- University of Colorado Sea Level Research Group (2018)

C-ROADS calibrates to projected values provided by the following sources:

- Network for Greening the Financial System (2023)
  - GCAM 6.0 (U.S.)
  - MESSAGEix-GLOBIOM 1.1-M-R12 (IIASA)
  - REMIND-MAgPIE 3.2-4.6 (Germany)
- SSP Version 2.0 scenarios (2018 - Available at: https://tntcat.iiasa.ac.at/SspDb)
  - Netherlands Environmental Assessment Agency (PBL). Integrated Model to Assess the Global Environment (IMAGE): Detlef van Vuuren, David Gernaat, Elke Stehfest
  - International Institute for Applied Systems Analysis (IIASA). Model for Energy Supply Strategy Alternatives and their General Environmental Impact - GLobal BIOsphere Management (MESSAGE-GLOBIOM): Keywan Riahi, Oliver Fricko, Petr Havlik
  - National Institute for Environmental Studies (NIES). Asia-Pacific Integrated Model (AIM): Shinichiro Fujimori
  - Pacific Northwest National Laboratory (PNNL). Global Change Assessment Model (GCAM): Kate Calvin and Jae Edmonds
  - Potsdam Institute for Climate Impact Research (PIK). REMIND-MAGPIE: Elmar Kriegler, Alexander Popp, Nico Bauer
  - European Institute on Economics and the Environment (EIEE). World Induced Technical Change Hybrid-GLobal BIOsphere Management (WITCH-GLOBIOM): Massimo Tavoni, Johannes Emmerling

Importing as data variables, C-ROADS assesses the GHG concentrations and temperature change projections given various emissions projections for model validation. Accordingly, there are necessary files, generated from data models, which must accompany the model. We test the model against the NGFS net emissions projections for their 6 scenarios. Reliably, for each scenario, the model captures the key dynamics of the NGFS models.

Although outdated now, we ran comparable assessments against all of the Shared Socioeconomic Pathway (SSP) of the IPCC's AR5 scenarios. Comparisons were against the output of 6 models for 5 SSP scenarios, each with up to 6 radiative forcing options, i.e., 1.9, 2.6, 3.4, 4.5, 6.0, and Baseline. Reliably, for each SSP storyline and RF level, the model captures the key dynamics of the SSP models.

Land Calibration

Land use change is calibrated based on the Land Use Harmonization (LUH2) data prepared for the Climate Research Program Coupled Model Intercomparison Project (CMIP6). Our output for each land type strongly aligns with historic data. However, our projections suggest more farmland and less forest than do the LUH projections and those of the NGFS models. The differences are due to our accounting for the temperature effect on reducing crop yield, which translates to more farmland expansion to meet food demands. The other models do not account for that feedback.

References

Asadoorian, M., Sarofim, C., Reilly, J., Paltsev, S., Forest, C. (2006) Historical Anthropogenic Emissions Inventories for Greenhouse Gases and Major Criteria Pollutants.

Massachusetts Institute of Technology (MIT) Joint Program on the Science and Policy of Global Change Technical Note No. 8. globalchange.mit.edu/files/document/MITJPSPGC_TechNote8.pdf.

Bernie, D., Lowe, J., Tyrrell, T., Legge, O. (2010) Influence of Mitigation Policy on Ocean Acidification. Geophysical Research Letters, 37:L15704.

Bolin, B. (1986) Requirements for a Satisfactory Model of the Global Carbon Cycle and Current Status of Modeling Efforts, in Trabalka, J. and Reichle, D (eds), The Changing Carbon Cycle: A Global Analysis. New York: Springer.

Björkstrom, A. (1986) One-Dimensional and Two-Dimensional Ocean Models for Predicting the Distribution of CO_2 Between the Ocean and the Atmosphere, in Trabalka, J. and Reichle, D (eds), The Changing Carbon Cycle: A Global Analysis. New York: Springer.

Brehmer, B. (1989) Feedback Delays and Control in Complex Dynamic Systems, in Miling, P. and E. Zahn (eds.), Computer Based Management of Complex Systems. Berlin: Springer Verlag, 189-196.

Bullister, J. (2009) NOAA/PMEL. Atmospheric CFC, CCl4, and SF_6 history update, retrieved 10/27/2009 from cdiac.ornl.gov/oceans/new_atmCFC.html.

Caldecott, Ben, Lomax, Guy, & Workman, Max. (2015). Stranded Carbon Assets and Negative Emission Technologies (Working Paper). University of Oxford Stranded Assets Programme. Retrieved from http://www.smithschool.ox.ac.uk/research-programmes/stranded-assets/Stranded%20Carbon%20Assets%20and%20NETs%20-%2006.02.15.pdf

Clarke, L., J. Edmonds, H. Jacoby, H. Pitcher, J. Reilly, R. Richels.(2007). Scenarios of Greenhouse Gas Emissions and Atmospheric Concentrations. Sub-report 2.1A of Synthesis and Assessment Product 2.1 by the U.S. Climate Change Science Program and the Subcommittee on Global Change Research. Department of Energy, Office of Biological & Environmental Research, Washington, 7 DC., USA, 154 pp.

Clarke, L., Edmonds, J., Krey, V., Richels, R., Rose, S., Tavoni, M. (2009) International Climate Policy Architectures: Overview of the EMF 22 International Scenarios. Energy Economics, 31:S64–S81.

Corell, R., Lee, K., Stern, P. (2009) Informing Decisions in a Changing Climate. National Research Council, Washington, DC: National Academies Press. nap.edu.

Daniel, J., Velders, G., et al. (2007) “Halocarbon Scenarios, Ozone Depletion Potentials, and Global Warming Potentials.” Ch. 8 in Scientific Assessment of Ozone Depletion: 2006. WMO (World Meteorological Organization) Global Ozone Research and Monitoring Project. Report 50, Geneva, 2007); www.esrl.noaa.gov/csd/assessments/ozone/2006/chapters/chapter8.pdf.

Den Elzen et al. (2005) Analysing countries’ contribution to climate change: scientific and policy-related choices. Environmental Science & Policy 8 614–636.

Energy Information Administration (EIA). (2008) International Energy Outlook 2008 (IEO_2008). Department of Energy’s Report #: DOE/EIA-0484(2008).

EDGAR (Emissions Database for Global Atmospheric Research) Community GHG Database (a collaboration between the European Commission, Joint Research Centre (JRC), the International Energy Agency (IEA), and comprising IEA-EDGAR CO_2, EDGAR CH_4, EDGAR N_2O, EDGAR F-GASES version 7.0, (2022) European Commission, JRC (Datasets). The complete citation of the EDGAR Community GHG Database is available in the 'Sources and References' section.

Fiddaman. T. (1997) Feedback Complexity in Integrated Climate-Economy Models. Ph.D. Dissertation, Massachusetts Institute of Technology.

Food and Agriculture Organization of the United Nations (FAO). Last updated February 8, 2022. . Forrester, J. W. Industrial Dynamics. (1961) MIT Press: Cambridge, MA.

Friedlingstein, P., Cox, P., Betts, R., Bopp, L., von Bloh, W., Brovkin, V., Cadule, et al. (2006) Climate-Carbon Cycle Feedback Analysis: Results from the C4MIP Model Intercomparison. Journal of Climate, 19:3337–3353.

Fujino, J., R. Nair, M. Kainuma, T. Masui, Y. Matsuoka, (2006). Multi-gas mitigation analysis on stabilization scenarios using AIM global model. Multigas Mitigation and Climate Policy. The Energy Journal Special Issue.

Fung, I. (1991) “Models of Oceanic and Terrestrial Sinks of Anthropogenic CO_2: A Review of the Contemporary Carbon Cycle” in Oremland, R. (ed.) Biogeochemistry of Global Change. New York: Chapman & Hall.

Global Carbon Budget (GCB). (2024). Friedlingstein, P., O'Sullivan, M., Jones, M. W., Andrew, R. M., Hauck, J., Landschützer, P., Le Quéré, C., Li, H., Luijkx, I. T., Olsen, A., Peters, G. P., Peters, W., Pongratz, J., Schwingshackl, C., Sitch, S., Canadell, J. G., Ciais, P., Jackson, R. B., Alin, S. R., Arneth, A., Arora, V., Bates, N. R., Becker, M., Bellouin, N., Berghoff, C. F., Bittig, H. C., Bopp, L., Cadule, P., Campbell, K., Chamberlain, M. A., Chandra, N., Chevallier, F., Chini, L. P., Colligan, T., Decayeux, J., Djeutchouang, L. M., Dou, X., Duran Rojas, C., Enyo, K., Evans, W., Fay, A. R., Feely, R. A., Ford, D. J., Foster, A., Gasser, T., Gehlen, M., Gkritzalis, T., Grassi, G., Gregor, L., Gruber, N., Gürses, Ö., Harris, I., Hefner, M., Heinke, J., Hurtt, G. C., Iida, Y., Ilyina, T., Jacobson, A. R., Jain, A. K., Jarníková, T., Jersild, A., Jiang, F., Jin, Z., Kato, E., Keeling, R. F., Klein Goldewijk, K., Knauer, J., Korsbakken, J. I., Lauvset, S. K., Lefèvre, N., Liu, Z., Liu, J., Ma, L., Maksyutov, S., Marland, G., Mayot, N., McGuire, P. C., Metzl, N., Monacci, N. M., Morgan, E. J., Nakaoka, S., Neill, C., Niwa, Y., Nützel, T., Olivier, L., Ono, T., Palmer, P. I., Pierrot, D., Qin, Z., Resplandy, L., Roobaert, A., Rosan, T. M., Rödenbeck, C., Schwinger, J., Smallman, T. L., Smith, S. M., Sospedra-Alfonso, R., Steinhoff, T., Sun, Q., Sutton, A. J., Séférian, R., Takao, S., Tatebe, H., Tian, H., Tilbrook, B., Torres, O., Tourigny, E., Tsujino, H., Tubiello, F., van der Werf, G., Wanninkhof, R., Wang, X., Yang, D., Yang, X., Yu, Z., Yuan, W., Yue, X., Zaehle, S., Zeng, N., and Zeng, J.: Global Carbon Budget 2024, Earth Syst. Sci. Data, https://essd.copernicus.org/preprints/essd-2024-519, 2024.

Global Forest Watch. (2024). Global burned Global Annual Tree Cover Loss from Fires, 2001 - 2023. (Accessed 2024).

Global Wildfire Information System. (2024).Global Monthly Burned Area, 2002 - 2023.. (Accessed 2024).

Goddard Institute for Space Studies (GISS) (2024) GISTEMP4 Global Mean Estimates based on Land and Ocean Data 1880-2023.

Goudriaan, J. and Ketner, P. (1984) A Simulation Study for the Global Carbon Cycle, Including Man's Impact on the Biosphere. Climatic Change, 6:167-192.

Gütschow, J.; Busch, D.; Pflüger, M. (2024): The PRIMAP-hist national historical emissions time series v2.6 (1750-2023). zenodo. doi:10.5281/zenodo.13752654.

Gütschow, J.; Jeffery, L.; Gieseke, R.; Gebel, R.; Stevens, D.; Krapp, M.; Rocha, M. (2016): The PRIMAP-hist national historical emissions time series, Earth Syst. Sci. Data, 8, 571-603, https://dx.doi.org/10.5194/essd-8-571-2016.

Hansen, J., Nazarenko, L., et al. (2005) Earth's energy imbalance: Confirmation and Implications. Science, 308:1431-1435. www.data.giss.nasa.gov.

Hansen, J., Sato, M., et al. (2005) Efficacy of Climate Forcings. Journal of Geophysical Research, 110.

Hansen, J., Sato, M., Lacis, A., Ruedy, R., Tegen, I. & Mathews, E. (1998) Climate Forcings in the Industrial Era. Proc of the Nat Acad of Sci, 95:12753-12758.

Hijioka, Y., Y. Matsuoka, H. Nishimoto, M. Masui, and M. Kainuma (2008). Global GHG emissions scenarios under GHG concentration stabilization targets. Journal of Global Environmental Engineering 13, 97-108.

Houghton, R. A., and A. A. Nassikas (2017), Global and regional fluxes of carbon from land use and land cover change 1850–2015, Global Biogeochem. Cycles, 31.doi:10.1002/2016GB005546.

Humpenöder, F., Popp, A., Dietrich, J. P., Klein, D., Lotze-Campen, H., Markus Bonsch, … Müller, C. (2014). Investigating afforestation and bioenergy CCS as climate change mitigation strategies. Environmental Research Letters, 9(6), 064029. https://doi.org/10.1088/1748-9326/9/6/064029

Intergovernmental Panel on Climate Change (IPCC). (2023): Summary for Policymakers. In: Climate Change 2023: Synthesis Report.A Report of the Intergovernmental Panel on Climate Change. Contribution of Working Groups I, II and III to the Sixth Assessment Report of the Intergovernmental Panel on Climate Change [Core Writing Team, H. Lee and J. Romero (eds.)]. IPCC, Geneva, Switzerland, (in press).

IPCC. (2021): Climate Change 2021: The Physical Science Basis. Contribution of Working Group I to the Sixth Assessment Report of the Intergovernmental Panel on Climate Change[Masson-Delmotte, V., P. Zhai, A. Pirani, S.L. Connors, C. Péan, S. Berger, N. Caud, Y. Chen, L. Goldfarb, M.I. Gomis, M. Huang, K. Leitzell, E. Lonnoy, J.B.R. Matthews, T.K. Maycock, T. Waterfield, O. Yelekçi, R. Yu, and B. Zhou (eds.)]. Cambridge University Press, Cambridge, United Kingdom and New York, NY, USA, In press, doi:10.1017/9781009157896.

IPCC. (2021): AR6 WG1, Chapter 5. Canadell, J.G., P.M.S. Monteiro, M.H. Costa, L. Cotrim da Cunha, P.M. Cox, A.V. Eliseev, S. Henson, M. Ishii, S. Jaccard, C. Koven, A. Lohila, P.K. Patra, S. Piao, J. Rogelj, S. Syampungani, S. Zaehle, and K. Zickfeld, 2021: Global Carbon and other Biogeochemical Cycles and Feedbacks. In Climate Change 2021: The Physical Science Basis. Contribution of Working Group I to the Sixth Assessment Report of the Intergovernmental Panel on Climate Change [Masson-Delmotte, V., P. Zhai, A. Pirani, S.L. Connors, C. Péan, S. Berger, N. Caud, Y. Chen, L. Goldfarb, M.I. Gomis, M. Huang, K. Leitzell, E. Lonnoy, J.B.R. Matthews, T.K. Maycock, T. Waterfield, O. Yelekçi, R. Yu, and B. Zhou (eds.)]. Cambridge University Press, Cambridge, United Kingdom and New York, NY, USA, pp. 673–816, doi: 10.1017/9781009157896.007.

IPCC. (2021): AR6 WG1, Chapter 6. Szopa, S., V. Naik, B. Adhikary, P. Artaxo, T. Berntsen, W.D. Collins, S. Fuzzi, L. Gallardo, A. Kiendler-Scharr, Z. Klimont, H. Liao, N. Unger, and P. Zanis, 2021: Short-Lived Climate Forcers. In Climate Change 2021: The Physical Science Basis. Contribution of Working Group I to the Sixth Assessment Report of the Intergovernmental Panel on Climate Change [Masson-Delmotte, V., P. Zhai, A. Pirani, S.L. Connors, C. Péan, S. Berger, N. Caud, Y. Chen, L. Goldfarb, M.I. Gomis, M. Huang, K. Leitzell, E. Lonnoy, J.B.R. Matthews, T.K. Maycock, T. Waterfield, O. Yelekçi, R. Yu, and B. Zhou (eds.)]. Cambridge University Press, Cambridge, United Kingdom and New York, NY, USA, pp. 817–922, doi: 10.1017/9781009157896.008.

IPCC. (2021): AR6 WG1, Chapter 7. Forster, P., T. Storelvmo, K. Armour, W. Collins, J.-L. Dufresne, D. Frame, D.J. Lunt, T. Mauritsen, M.D. Palmer, M. Watanabe, M. Wild, and H. Zhang, 2021: The Earth's Energy Budget, Climate Feedbacks, and Climate Sensitivity. In Climate Change 2021: The Physical Science Basis. Contribution of Working Group I to the Sixth Assessment Report of the Intergovernmental Panel on Climate Change [Masson-Delmotte, V., P. Zhai, A. Pirani, S.L. Connors, C. Péan, S. Berger, N. Caud, Y. Chen, L. Goldfarb, M.I. Gomis, M. Huang, K. Leitzell, E. Lonnoy, J.B.R. Matthews, T.K. Maycock, T. Waterfield, O. Yelekçi, R. Yu, and B. Zhou (eds.)]. Cambridge University Press, Cambridge, United Kingdom and New York, NY, USA, pp. 923–1054, doi: 10.1017/9781009157896.009.

IPCC. (2021): AR6 Technical Summary. Arias, P.A., N. Bellouin, E. Coppola, R.G. Jones, G. Krinner, J. Marotzke, V. Naik, M.D. Palmer, G.-K. Plattner, J. Rogelj, M. Rojas, J. Sillmann, T. Storelvmo, P.W. Thorne, B. Trewin, K. Achuta Rao, B. Adhikary, R.P. Allan, K. Armour, G. Bala, R. Barimalala, S. Berger, J.G. Canadell, C. Cassou, A. Cherchi, W. Collins, W.D. Collins, S.L. Connors, S. Corti, F. Cruz, F.J. Dentener, C. Dereczynski, A. Di Luca, A. Diongue Niang, F.J. Doblas-Reyes, A. Dosio, H. Douville, F. Engelbrecht, V. Eyring, E. Fischer, P. Forster, B. Fox-Kemper, J.S. Fuglestvedt, J.C. Fyfe, N.P. Gillett, L. Goldfarb, I. Gorodetskaya, J.M. Gutierrez, R. Hamdi, E. Hawkins, H.T. Hewitt, P. Hope, A.S. Islam, C. Jones, D.S. Kaufman, R.E. Kopp, Y. Kosaka, J. Kossin, S. Krakovska, J.-Y. Lee, J. Li, T. Mauritsen, T.K. Maycock, M. Meinshausen, S.-K. Min, P.M.S. Monteiro, T. Ngo-Duc, F. Otto, I. Pinto, A. Pirani, K. Raghavan, R. Ranasinghe, A.C. Ruane, L. Ruiz, J.-B. Sallée, B.H. Samset, S. Sathyendranath, S.I. Seneviratne, A.A. Sörensson, S. Szopa, I. Takayabu, A.-M. Tréguier, B. van den Hurk, R. Vautard, K. von Schuckmann, S. Zaehle, X. Zhang, and K. Zickfeld, 2021: Technical Summary. In Climate Change 2021: The Physical Science Basis. Contribution of Working Group I to the Sixth Assessment Report of the Intergovernmental Panel on Climate Change [Masson-Delmotte, V., P. Zhai, A. Pirani, S.L. Connors, C. Péan, S. Berger, N. Caud, Y. Chen, L. Goldfarb, M.I. Gomis, M. Huang, K. Leitzell, E. Lonnoy, J.B.R. Matthews, T.K. Maycock, T. Waterfield, O. Yelekçi, R. Yu, and B. Zhou (eds.)]. Cambridge University Press, Cambridge, United Kingdom and New York, NY, USA, pp. 33–144, doi:10.1017/9781009157896.002.

IPCC. (2021): AR6 Summary for Policymakers. In: Climate Change 2021: The Physical Science Basis. Contribution of Working Group I to the Sixth Assessment Report of the Intergovernmental Panel on Climate Change [Masson-Delmotte, V., P. Zhai, A. Pirani, S.L. Connors, C. Péan, S. Berger, N. Caud, Y. Chen, L. Goldfarb, M.I. Gomis, M. Huang, K. Leitzell, E. Lonnoy, J.B.R. Matthews, T.K. Maycock, T. Waterfield, O. Yelekçi, R. Yu, and B. Zhou (eds.)]. Cambridge University Press, Cambridge, United Kingdom and New York, NY, USA, pp. 3–32, doi:10.1017/9781009157896.001.

International Energy Agency (IEA). (2022) World Energy Outlook (WEO).

John, J.G. , A. M. Fiore, V. Naik, L.W. Horowitz, and J. P. Dunne. (2012). Climate versus emission drivers of methane lifetime against loss by tropospheric OH from 1860-2100. Atmos. Chem. Phys., 12, 12021-12036.

Jones, M. W., Veraverbeke, S., Andela, N., Doerr, S. H., Kolden, C., Mataveli, G., Pettinari, M. L., Le Quere, C., Rosan, T. M., Van Der Werf, G. R., Van Wees, D., & Abatzoglou, J. T. (2024). Global rise in forest fire emissions linked to climate change in the extratropics. *Science, 386*(6719), eadl5889.

Joos, F., Prentice, I., Sitch, S., Meyer, R., Hooss, G., Plattner, G., Gerber, S. and Hasselmann, K. (2001) Global Warming Feedbacks on Terrestrial Carbon Uptake Under the Intergovernmental Panel on Climate Change (IPCC) Emissions Scenarios. Global Biogeochemical Cycles, 15:891- 908.

Kheshgi, H. and Jain, A. (2003) Projecting Future Climate Change: Implications of Carbon Cycle Model Intercomparisons. Global Biogeochemical Cycles, 17:1047, doi:10.1029/2001GB001842.

Kleinmuntz, D. and J. Thomas. (1987). The Value of Action and Inference in Dynamic Decision-Making. Organization Behavior and Human Decision Processes 39(3), 341-364.

Knorr, W., et al. (2016). Demographic controls of future global fire risk. *Nature Climate Change, 6*(8), 781-785.

Knutti, R., S. Kra¨henmann, D. J. Frame, and M. R. Allen (2008), Comment on Heat capacity, time constant, and sensitivity of Earth,s climate system, by S. E. Schwartz, J. Geophys. Res., 113, D15103, doi:10.1029/2007JD009473.

Koornneef, Joris, van Breevoort, Pieter, Hamelinck, Carlo, Hendriks, Chris, Hoogwijk, Monique, Koop, Klaas, & Koper, Michele. (2011). Potential for Biomass and Carbon Dioxide Capture and Storage. EcoFys for IEA GHG. Retrieved from https://www.eenews.net/assets/2011/08/04/document_cw_01.pdf

Lange, S., et al. (2020). Projecting exposure to extreme climate impact events across six event categories and three spatial scales. *Earth's Future, 8*(12), e2020EF001616.

Lenton, T. M. (2010). The potential for land-based biological CO_2 removal to lower future atmospheric CO_2 concentration. Carbon Management, 1(1), 145–160. https://doi.org/10.4155/cmt.10.12

Maddison, A., (2008) Historical Statistics for the World Economy: 1-2006 AD. Conference Board and Groningen Growth and Development Centre, Total Economy Database, www.ggdc.net/MADDISON/oriindex.htm.

Manne, A. and R. Richels. (2004) MERGE: An Integrated Assessment Model for Global Climate Change.

Malone, T., Abelson, H., Karger, D., Klein, M., Sterman, J. (2011) The Climate CoLab. climatecolab.org.

Mayer, M., Hyman, R., Harnisch, J., Reilly, J. (2000) Emissions Inventories and Time Trends for Greenhouse Gases and other Pollutants. Massachusetts Institute of Technology (MIT) Joint Program on the Science and Policy of Global Change, Technical Note No. 1. globalchange.mit.edu/files/document/MITJPSPGC_TechNote1.pdf.

M. Meinshausen, S. C. B. Raper, and T. M. L. Wigley. (2011). Emulating coupled atmosphere-ocean and carbon cycle models with a simpler model, MAGICC6 – Part 1: Model description and calibration: Atmos. Chem. Phys., 11, 1417–1456. http://www.atmos-chem-phys.net/11/1417/2011/acp-11-1417-2011.pdf.

Mclaren, D. (2012). A comparative global assessment of potential negative emissions technologies. Process Safety and Environmental Protection, 90, 489–500. https://doi.org/10.1016/j.psep.2012.10.005.

Meinshausen, M., Raper, S., Wigley, T. (2008) Emulating IPCC AR4 atmosphere-ocean and carbon cycle models for projecting global-mean, hemispheric and land/ocean temperatures: MAGICC 6.0. Atmospheric Chemistry and Physics Discussions, 8:6153-6272. www.atmos-chem-phys-discuss.net/8/6153/2008/.

Meinshausen, M., N. Meinshausen, W. Hare, S.C.B. Raper, K. Frieler, R. Knutti, D.J. Frame, and M.R. Allen. (2009). Greenhouse-gas emission targets for limiting global warming to 20C. Nature. 458: 1158-1163.

Meinshausen, M. and S. Smith et al. (2011). The RCP GHG concentrations and their extension from 1765 to 2300", DOI 10.1007/s10584-011-0156-z, Climatic Change.

Meadows, D. H., Meadows, D. L. Randers, J. Behrens, W. W. The Limits To Growth. (1972) Universe Books: New York, NY.

Miller, R.L., G.A. Schmidt, L.S. Nazarenko, et al, 2015: CMIP5 historical simulations (1850-2012) with GISS ModelE2. J. Adv. Model. Earth Syst., 6, no. 2, 441-477, doi:10.1002/2013MS000266.

Morecroft, J. and Sterman, J. (1994) Modeling for Learning Organizations. Portland, OR: Productivity Press.

Nakicenovic, N., Swart, R. Eds. (2000) Special Report on Emissions Scenarios. Cambridge University Press: Cambridge, United Kingdom.

National Oceanic & Atmospheric Administration (NOAA). (2025). CO_2: Lan, X., Tans, P. and K.W. Thoning: Trends in globally-averaged CO_2 determined from NOAA Global Monitoring Laboratory measurements. Version 2025-04 https://doi.org/10.15138/9N0H-ZH07. CH_4, N_2O, and SF_6: Lan, X., K.W. Thoning, and E.J. Dlugokencky: Trends in globally-averaged CH_4, N_2O, and SF_6 determined from NOAA Global Monitoring Laboratory measurements. Version 2025-04, https://doi.org/10.15138/P8XG-AA10.

National Research Council. (2015). Climate Intervention: Carbon Dioxide Removal and Reliable Sequestration. Retrieved from https://www.nap.edu/catalog/18805/climate-intervention-carbon-dioxide-removal-and-reliable-sequestration.

Newbold S.C. and Daigneault A. (2008) Climate Response Uncertainty and the Expected Benefits of Greenhouse Gas Emissions Reductions. US EPA Working Paper # 08-06.

Nordhaus, W. and G. Yohe. (1983) Future Carbon Dioxide Emissions from Fossil Fuels. In Changing Climate: Report of the Carbon Dioxide Assessment Committee, ed. Washington, DC: National Academy Press.

Nordhaus, W. D. (1992) The "DICE" Model: Background and Structure of a Dynamic Integrated Climate-Economy Model of the Economics of Global Warming. Cowles Foundation for Research in Economics at Yale University, Discussion Paper No. 1009.

Nordhaus, W. D. (1994) Managing the Global Commons. Cambridge, MA: MIT Press. Nordhaus W.D. and Boyer, (2000) Warming the World: Economic Models of Global Warming Cambridge, MA: MIT Press.

Oeschger, H., Siegenthaler, U., et al. (1975) A Box Diffusion Model to Study the Carbon Dioxide Exchange in Nature. Tellus, 27(2):167-192.

Olivier, J. and Berdowski, J. (2001) Global emissions sources and sinks. In: Berdowski, J., Guicherit, R. and Heij, B. (eds.) The Climate System, 33-78. A.A. Balkema Publishers/Swets & Zeitlinger Publishers, Lisse, The Netherlands. ISBN 90 5809 255 0.

Rahmstorf, S. (2007) Sea-Level Rise A Semi-Empirical Approach to Projecting Future Sea Level Rise. Science, 315:368-370.

Randall, D. 2010. The Evolution of Complexity In General Circulation Models. www.aip.org/history/sloan/gcm/intro.html

Riahi, K. Gruebler, A. and Nakicenovic N.: 2007. Scenarios of long-term socio-economic and environmental development under climate stabilization. Technological Forecasting and Social Change 74, 7, 887-935.

Rotmans, J. (1990) IMAGE: An Integrated Model to Assess the Greenhouse Effect. Boston: Kluwer Academic Publishers.

Schwartz, S.E. 2007. Heat Capacity, Time Constant, and Sensitivity of Earth's Climate System. Journal of Geophysical Research.

Schneider, S.H., and S.L. Thompson. 1981. Atmospheric CO_2 and Climate: Importance of the Transient Response. Journal of Geophysical Research 86: 3135-3147.

Smith, S.J. and T.M.L. Wigley, 2006. Multi-Gas Forcing Stabilization with the MiniCAM. Energy Journal (Special Issue #3) pp 373-391.

Socolow, R., Lam, S. (2007) Good Enough Tools for Global Warming Policy-Making. Philosophical Transactions of the Royal Society A, 365:897–934. SSP Database (Shared Socioeconomic Pathways) - Version 1.1. Available at: https://tntcat.iiasa.ac.at/SspDb.

Sterman, J. (1994) Learning In and About Complex Systems. System Dynamics Review, 10(2-3): 291-330.

Sterman, J. (2000) Business Dynamics. Irwin McGraw Hill: Boston, MA.

Sterman, J. (2008) Risk Communication on Climate: Mental Models and Mass Balance. Science, 322:532-533.
Sterman, J. (2011) Communicating Climate Change Risks in a Skeptical World. Climatic Change, 108. DOI 10.1007/s10584-011-0189-3.

Sterman, J. and Booth Sweeney, L. (2002) Cloudy Skies: Assessing Public Understanding of Climate Change. System Dynamics Review, 18(2):207-240.

Sterman, J. & Booth Sweeney, L., (2007) Understanding Public Complacency About Climate Change: Adults' Mental Models of Climate Change Violate Conservation of Matter. Climatic Change, 80:213-238.

Sterman, J., Fiddaman, T., Franck, T., Jones, A., McCauley, S., Rice, P., Sawin, E., Siegel, L. (2011) World Climate: A Role-Play Simulation of Global Climate Negotiations. Working Paper, MIT Sloan School of Management, jsterman.scripts.mit.edu/docs/World Climate.pdf.

Stern, D., and Kaufmann, R. (1998) Annual Estimates of Global Anthropogenic Methane Emissions: 1860-1994. Trends Online: A Compendium of Data on Global Change. Carbon Dioxide Information Analysis Center, Oak Ridge National Laboratory, U.S. Department of Energy, Oak Ridge, Tenn., doi: 10.3334/CDIAC/tge.001. cdiac.ornl.gov/trends/meth/ch4.htm.

UNEP (2010) The Emissions Gap Report. UN Environment Programme. Available at www.unep.org/publications/ebooks/emissionsgapreport/.

Tsuneyuki Morita. (1999) Emissions Scenario Database prepared for IPCC Special Report on Emissions Scenarios convened by Dr. Nebosja Nakicenovic. The database was downloaded at http://www.cger.nies.go.jp/scenario/download/GHGSDB_CompleteEdition.zip.

United Nations, Department of Economic and Social Affairs, Population Division (2024). World Population Prospects: The 2024 Revision.

Van Aardenne, J., Dentener, F., Olivier, J., Klein Goldewijk, C. and Lelieveld, J. (2001) A 1 x 1 degree resolution dataset of historical anthropogenic trace gas emissions for the period 1890- 1990. Global Biogeochemical Cycles, 15(4): 909-928.

van Vuuren, D. P., Deetman, S., van Vliet, J., van den Berg, M., van Ruijven, B. J., & Koelbl, B. (2013). The role of negative CO_2 emissions for reaching 2 °C--insights from integrated assessment modelling. Climatic Change; Dordrecht, 118(1), 15–27. https://doi.org/http://dx.doi.org.libproxy.tulane.edu:2048/10.1007/s10584-012-0680-5.

van Vuuren, D., M. den Elzen, P. Lucas, B. Eickhout, B. Strengers, B. van Ruijven, S. Wonink, R. van Houdt, 2007. Stabilizing greenhouse gas concentrations at low levels: an assessment of reduction strategies and costs. Climatic Change, doi:10.1007/s/10584-006-9172-9.

Vermeer, M. and S. Rahmstorf. 2009. Global sea level linked to global temperature. Proc of the Nat Acad of Sci. 106(51):21527-21532. www.pnas.org/cgi/doi/10.1073/pnas.0907765106.

Walker, S, Weiss, R., and Salameh, P. (2000) Reconstructed histories of the annual mean atmospheric mole fractions for the halocarbons CFC-11, CFC-12, CFC-113 and carbon tetrachloride. J. Geophysical Res., 105:14285-14296.

Weitzman, Martin L. 2009. On modeling and interpreting the economics of catastrophic climate change. Review of Economics and Statistics 91(1):1-19.

Wigley, T. (2008) MAGICC/SCENGEN 5.3: User Manual (V2). www.cgd.ucar.edu/cas/wigley/magicc/. Wise, MA, KV Calvin, AM Thomson, LE Clarke, B Bond-Lamberty, RD Sands, SJ Smith, AC Janetos, JA Edmonds. 2009. Implications of Limiting CO_2 Concentrations for Land Use and Energy. Science. 324:1183-1186. May 29, 2009.

World Resources Institute (WRI). 2016. CAIT output. http://cait.wri.org/historical/ Wullschleger, S., Post, W. et al. (1995) On the Potential for a CO_2 Fertilization Effect in Forests: Estimates of the Biotic Growth Factor Based on 58 Controlled-Exposure Studies. In Woodwell, G. & Mackenzie, F. (eds), Biotic Feedbacks in the Global Climatic System, New York: Oxford Univ. Press, 85-107.

Woolf, D., Amonette, J. E., Street-Perrott, F. A., Lehmann, J., & Joseph, S. (2010). Sustainable biochar to mitigate global climate change. Nature Communications, 1, 1. https://doi.org/10.1038/ncomms1053.

World Bank. 2024. World Development Indicators, 1960-2023. https://data.worldbank.org/indicator/NY.GDP.MKTP.PP.KD. Constant $ 2021 US (PPP).